

# Observations of gas flow in porous media using a light transmission technique

Laila Parker,<sup>1</sup> Rockie Yarwood,<sup>2</sup> and John Selker<sup>1</sup>

Received 4 March 2005; revised 8 September 2005; accepted 23 January 2006; published 16 May 2006.

[1] A novel technique for quantitative nondestructive study of two-dimensional disposition of gas phase in unsaturated porous media is presented. Carbon dioxide was pumped through a backlit 1 cm thick chamber packed with translucent sand, which was variably saturated with water containing the pH indicator dye methyl red. As the carbon dioxide dissolved in the pore water, lowering the pH and changing the dye color, a CCD camera captured images of the resultant changes in transmitted light. These digital image files were then processed using a series of calibrated steps to relate light intensity to dye attenuation, dye attenuation to solution pH, and solution pH to aqueous and gaseous carbon dioxide concentration. The final product was a series of false-color images showing the development of the gaseous carbon dioxide plume. Limitations were found that will require further development, including more attention to calibration of dye concentration versus observed transmission and investigation of dye solubility across the range of pH values employed. With refinement, this technique may prove to be a useful tool in studying the complexities of gas phase transport in variably saturated porous media.

**Citation:** Parker, L., R. Yarwood, and J. Selker (2006), Observations of gas flow in porous media using a light transmission technique, *Water Resour. Res.*, 42, W05501, doi:10.1029/2005WR004080.

## 1. Introduction

[2] The development of new experimental methods for observing gases in unsaturated porous media is an essential step toward improved understanding of gas phase transport which plays an important role in the hydrology, biology, and chemistry of natural unsaturated porous media. Here we describe a strategy to use the two-dimensional light transmission method (LTM) to observe gas transport in unsaturated media. A pH indicator dye was used to quantify carbon dioxide (CO<sub>2</sub>) concentration based on soluble CO<sub>2</sub> alteration of pH. The LTM is a quantitative noninvasive laboratory-based measurement approach to make observations of unsaturated zone processes including water and solute distribution, colloid transport, nonaqueous phase liquid flow, and interactions between water flow and microbial colonization [e.g., *Niemet and Selker*, 2001; *Weisbrod et al.*, 2003; *Schroth et al.*, 1998; *Yarwood et al.*, 2002]. To our knowledge, the LTM has not yet been applied to the observation of gas transport, but this application would be useful in its own right, and an important complement to the proven capabilities of these systems.

## 2. Methods

### 2.1. Chamber Preparation

[3] The pH indicator dye methyl red was used because its pH range approximates that of the CO<sub>2</sub>-water system (pH

7–3.9) and its color change, from yellow to red, is readily detectable by the human eye. Methyl red (0.005% w/v methyl red powder (Matheson, Coleman and Bell) in deionized water) was prepared in 10 L batches with 0.25 M KOH added to aid dissolution.

[4] The 50 × 50 × 1 cm chamber was packed with a 40/50 sieve-size silica sand [*Schroth et al.*, 1996] and prepared following the methods of *Niemet and Selker* [2001]. After saturation with the 0.005% methyl red solution, the chamber was drained to residual saturation, with a roughly 12 cm saturated capillary fringe along the bottom of the chamber. The upper boundary of the chamber was sealed with an aluminum cover to preclude escaped gas and eliminate evaporation from the sand's surface. CO<sub>2</sub> was sparged through water and pumped into the left-hand and out of the right-hand sparging stones, located 15 cm from the left and right chamber edges and 22 cm from the bottom of the chamber with gauged identical peristaltic pump heads (see Figure 1). Experiments lasted for 34 min at temperatures of 20°C ± 2 °C. Data from 3 experiments are presented here: experiment 1 was conducted with a gas flow rate of 40 mL h<sup>-1</sup>, while experiment 2 and 3 were conducted with a gas flow rate of 280 mL h<sup>-1</sup>.

[5] The predicted mass of CO<sub>2</sub> in the chamber was compared with the total mass added to the system at 3 min intervals. Added mass was computed as the product of time and flow rate, and does not account for gas removal from the outlet port. Predicted masses were separately calculated in both phases and then summed. Dissolved phase concentrations were multiplied by corresponding water content values, and resulting pixel values were summed to yield total dissolved phase CO<sub>2</sub> mass. Gas phase concentrations were multiplied by corresponding available pore volumes, which were computed by subtracting water content at each pixel from porosity ( $\eta = 0.348$ , from

<sup>1</sup>Department of Bioengineering, Oregon State University, Corvallis, Oregon, USA.

<sup>2</sup>Department of Crop and Soil Sciences, Oregon State University, Corvallis, Oregon, USA.

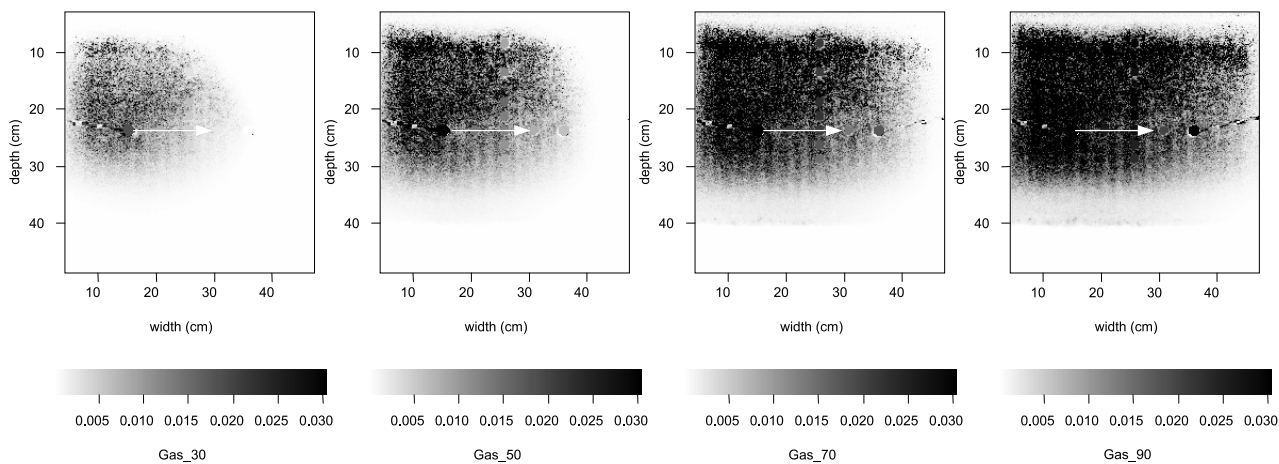


**Figure 1.** Images portraying the development of a plume of gaseous  $\text{CO}_2$  in experiment 3 at 9, 15, 21, and 27 min. Scale bar indicates  $[\text{CO}_2]_g$  in  $\text{mol L}^{-1}$ ; bull's-eyes mark gas inlet and outlet ports, and axes show depth and width in centimeters. Arrows show direction of gas flow.

packing data). Resulting values were summed to yield total gas phase  $\text{CO}_2$  mass.

## 2.2. Image Capture

[6] The light bank behind the translucent sand was illuminated during experiments as data images were captured at 18 s intervals by the camera, a liquid-cooled 16-bit, grayscale, 512 by 512 pixel charge coupled device (CCD)

imaging chip (Princeton Instruments), used with a Nikon 35 mm, f-1.4 aperture lens (Nikon Corporation). The camera's 500 nm wideband filter (70 nm spread) (model 57561, Oriel Instruments) provided sensitivity to the color change of the methyl red dye with pH. Images were saved in WinView software (Princeton Instruments) as arrays of 512 by 512 pixels (1 pixel  $\cong 1 \text{ mm}^2$  of chamber surface area). Each array was imported into Fortner Transform (version 3.4,

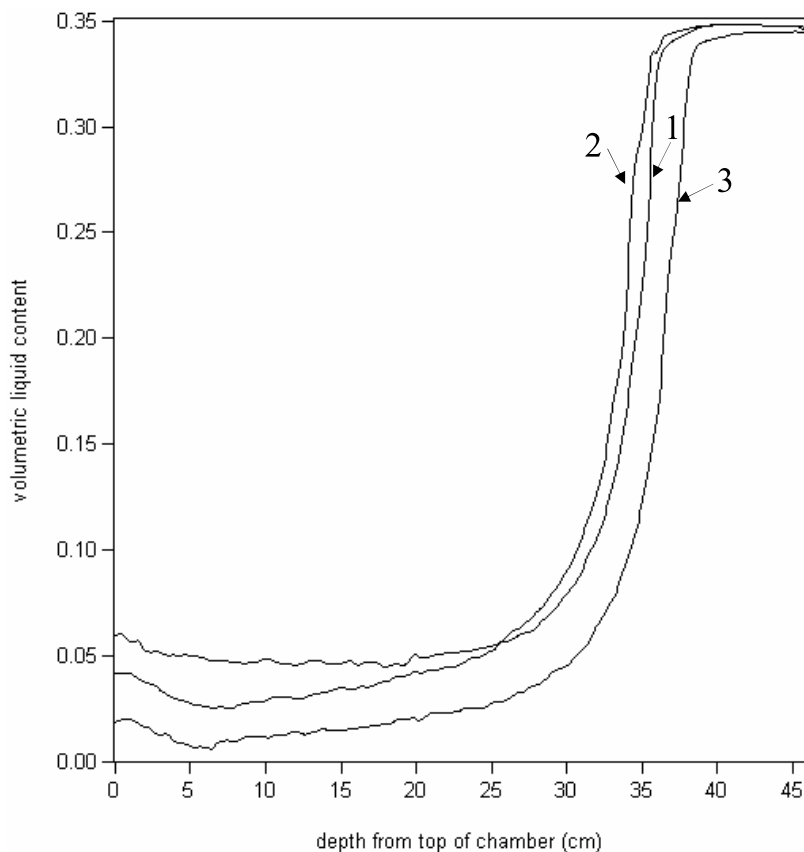


**Figure 2.** Volumetric liquid content profiles of experiments 1, 2, and 3. Profiles represent a vertical transect through the chamber at a point 7 cm from the left side of the chamber. The y axis represents volumetric liquid content ( $\theta$ ); the x axis represents depth from the top of the chamber.

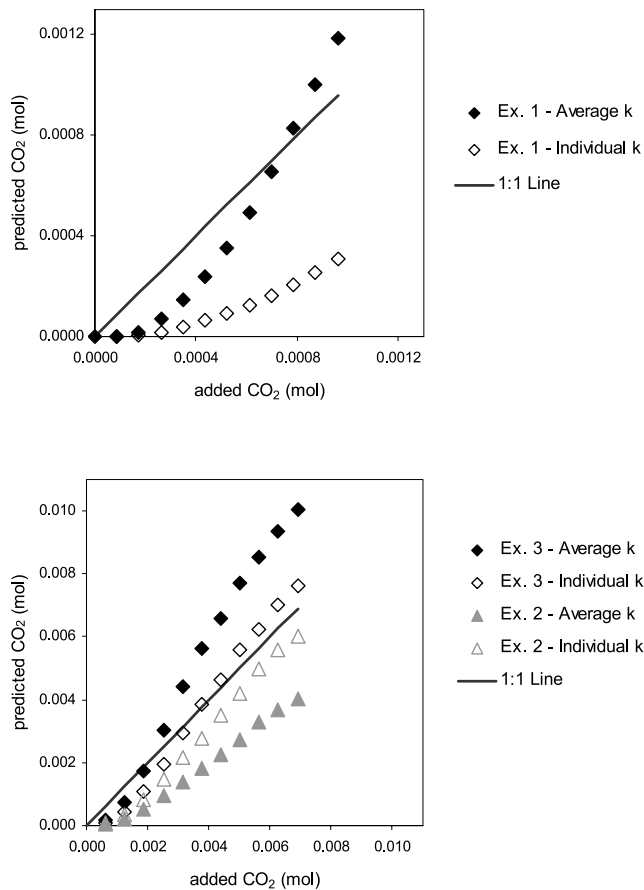


**Figure 3.** Mass balance analysis of predicted  $\text{CO}_2$ . Experiments are grouped by gas flow rate. Data points represent calculations made at 3 min intervals. Solid diamonds and shaded triangles show data computed using an averaged  $k$  value; open diamonds and open triangles show data computed with a  $k$  value individual to that experiment. The 1:1 line represents the mass added to the system.

Fortner Software LLC), and was processed via the equations described below on a pixel-by-pixel basis.

### 2.3. Image Processing

[7] Raw data were initially corrected for bias signal contributions as described by *Niemi and Selker* [2001], and image edges were trimmed, yielding a 467 by 435 pixel array (46.2 cm by 43.1 cm). Image processing, described below, sequentially transformed the raw data into (1) water content, (2) light attenuation due to dye, (3) pH, (4) dissolved ( $[\text{CO}_2]_l$ ) ( $\text{mol L}^{-1}$ ), and (5) gas phase ( $[\text{CO}_2]_g$ ) ( $\text{mol L}^{-1}$ ).

[8] 1. One image of water content prior to  $\text{CO}_2$  addition was created per experiment, after Model E described by *Niemi and Selker* [2001]. Water content was assumed to be constant throughout the duration of the  $\text{CO}_2$  trace experiment as the gas was humidified before being introduced to the chamber. Sample water content profiles are shown in Figure 2.

[9] 2. The change in transmitted light due to the effects of  $\text{CO}_2$  dissolution on dye color was expressed as a function of dye extinction coefficient and water content, using an equation developed by *Rockhold* [2002]. In a series of

dye visualization experiments in the chamber, *Rockhold* [2002] found that dye concentration could be determined from light attenuation through modification of Beer's law to account for nonlinear effects of water content on light attenuation, such that

$$\alpha = \left[ \frac{k}{\theta^{0.42}} \ln \left[ \frac{I}{I_0} \right] \right]^{1.35}, \quad (1)$$

where  $\theta$  is the volumetric liquid content,  $\alpha$  = dye extinction coefficient,  $I_0$  = pre- $\text{CO}_2$  addition pixel intensity,  $I$  = post- $\text{CO}_2$  addition pixel intensity, and  $k$  is a dye-specific constant. Assuming  $\text{CO}_2$  saturation ( $0.039 \text{ mol L}^{-1}$  at standard pressure) around the inlet, the  $k$  value was calibrated using  $\alpha = 5.9$  at  $\text{CO}_2$  saturation (computed using  $\text{CO}_2$ - $\alpha$  relationships described below) and averaged values of  $I$ ,  $I_0$  and  $\theta$  of 20 pixels around the inlet, where  $I$  represents the last image in an experiment. The concept of this approach was to find an area of the chamber that had definitely been exposed to pure  $\text{CO}_2$  for a period long enough to be at equilibrium liquid phase concentration. Using the least squares method, optimal  $k$  values were found for each experiment as follows: experiment 1,  $k = -1.62$ ; experiment 2,  $k = -2.04$ ; experiment 3,  $k = -1.83$ . For this paper, data was processed twice using both individual  $k$  values and an average  $k$  value of  $-1.94$  (from experiments 2 and 3).

[10] 3. A standard curve was created to relate dye attenuation to solution pH. Three replicates of sixteen 0.005% methyl red samples spanning pH 3.9–7.2 were measured for percent transmittance at 520 nm using a spectrophotometer (Spectronic 21, Bausch & Lomb). Sample pH was manipulated with drop-wise additions of hydrochloric acid and measured with a pH meter (model SA250, Orion Research). Attenuation was fit to measured transmittance by adjusting  $\alpha$  in Beer's law,

$$T = e^{-1.14\alpha}, \quad (2)$$

where 1.14 is the thickness (cm) of the cuvette used to measure transmittance and  $T$  is a fractional value of transmittance. The attenuation-pH data resembled the shape of the *van Genuchten* [1980] water retention function, thus the data were fit to an equation of this form using the least squares method, where  $p = \text{pH}$ , with fitting parameters  $r = 0.475$ ,  $s = 1$ ,  $a = 0.174$ ,  $n = 15.4$  and  $m = 0.94$ :

$$p = \frac{\left[ \left( \frac{s-r}{1-e^{-1.14\alpha}-r} \right)^{\frac{1}{n}} - 1 \right]^{\frac{1}{m}}}{a}. \quad (3)$$

The fit of this model to attenuation-pH data ( $R^2 = 0.84$ ) was impaired by the dye's tendency to flocculate at low pH, as is discussed in greater detail in the results and discussion section of this paper.

[11] 4. Considering  $\text{CO}_2$  as a nonreactive tracer, with a diffusion coefficient in water of  $1.6 \times 10^{-5} \text{ cm}^2/\text{s}$  [*Hillel*, 1998], and a film thickness of 0.01 cm (an upper bound based on the typical pore size being approximately 1/3 of the mean grain size), we can estimate that the gas and liquid phase  $\text{CO}_2$  concentrations equilibrate in less than two seconds, thus we take the equilibria to be instantaneous for the

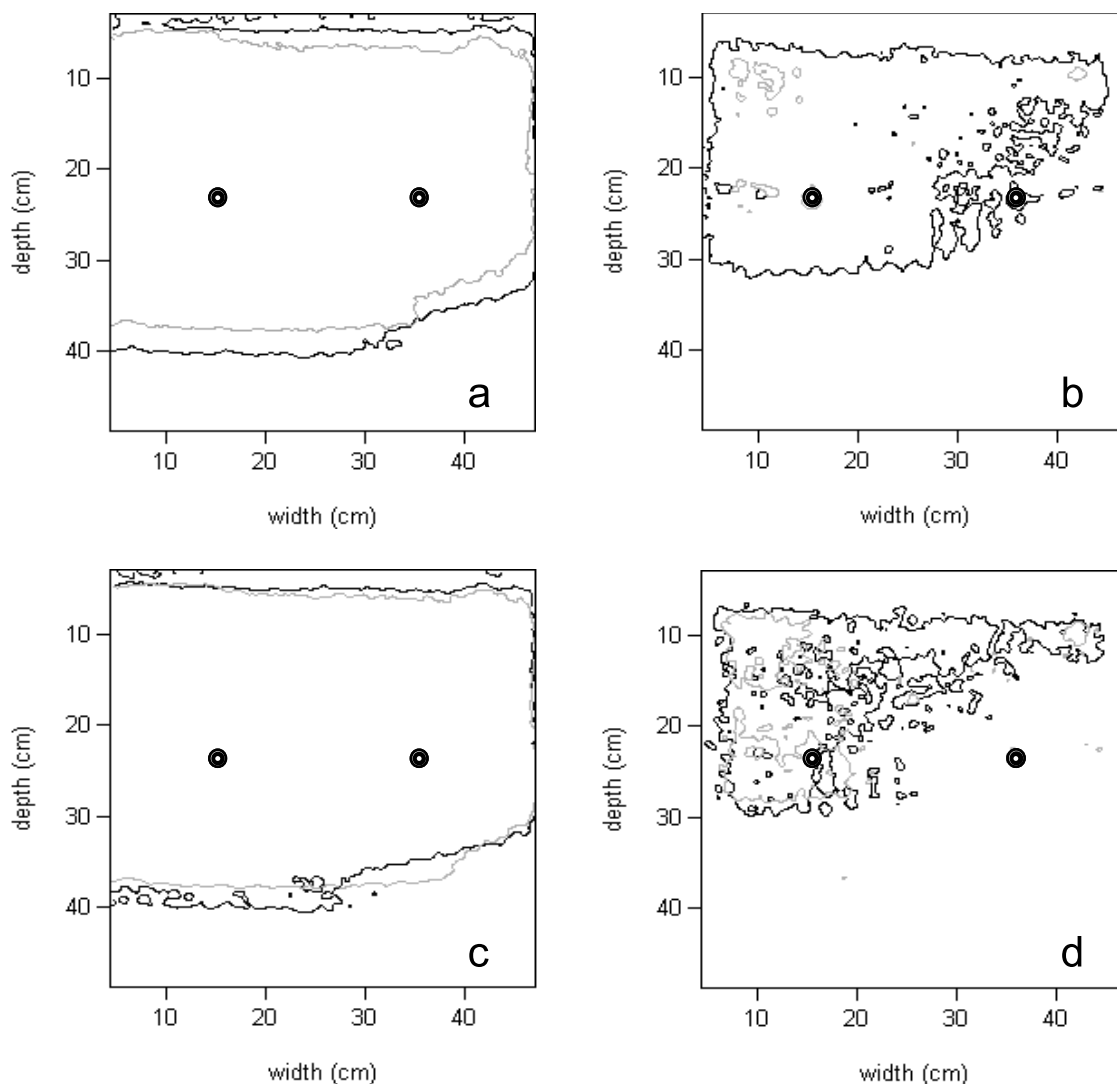


**Figure 4.** Contour images showing the extent of the plume at time = 30 min within which  $\text{CO}_2$  is at or above 5 and 75% saturation as follows: (a) 5% (average  $k$  value), (b) 75% (average  $k$  value), (c) 5% (individual  $k$  value), and (d) 75% (individual  $k$  value). Shaded lines represent data from experiment 2, and solid lines represent experiment 3. Bull's-eyes mark gas inlet and outlet ports, and axes show depth and width in centimeters.

purpose of these experiments. We can thus calculate  $[\text{CO}_2]_l$  from a given pH based on equilibrium equations describing the hydration and ionization reactions of  $\text{CO}_2$  in water, combined with the definition of pH and a value for the equilibrium constant  $K$  at  $20^\circ\text{C}$ ,  $K = 10^{-6.381}$  [Butler, 1982]. Hence we may compute the liquid phase concentration as

$$[\text{CO}_2]_l = \frac{10^{-2\text{pH}}}{K}. \quad (4)$$

[12] 5. Henry's law, describing the solubilization of gases into liquid, is used to calculate  $[\text{CO}_2]_g$  from  $[\text{CO}_2]_l$ , where  $K_H = 0.774$  [Butler, 1982],

$$[\text{CO}_2]_g = K_H [\text{CO}_2]_l. \quad (5)$$

Plume images were smoothed to minimize noise using the "Smooth Data" function in Transform, and contours

of  $\text{CO}_2$  gas concentration were generated from the images.

### 3. Results and Discussion

[13] Image processing produced a series of 120 images of gas phase and dissolved phase  $\text{CO}_2$  plumes. Examples of these false color images are shown in Figure 1; an entire series is viewable as Animation S1<sup>1</sup>. Note that the gas-filled pore space in the chamber did not become saturated with  $\text{CO}_2$  because the volume of introduced  $\text{CO}_2$  (154 mL) was smaller than the gas-filled pore volume ( $>500$  mL). An apparent detection threshold of about 0.0002 moles can be seen in Figure 3, which is about 5 ml at STP. Though we have not conclusively determined the source of this effect, this coincides with the volume of the tubing leading from

<sup>1</sup>Auxiliary material is available at <ftp://ftp.agu.org/apend/wr/2005/wr004080>.

the pump to the chamber, which due to its incorporation into the chamber could not be purged prior to the experiment.

[14] The predictions from the procedure are highly dependent on  $k$  values, the variability of which may be due to dye insolubility. Predicted CO<sub>2</sub> mass values from experiment 1 were closer to the 1:1 line when the averaged  $k$  value was used (Figure 3); the assumption of CO<sub>2</sub> saturation of the inlet area may have been inaccurate in this experiment where the gas flow rate was relatively low (40 mL h<sup>-1</sup>). In contrast, the individual  $k$  values yielded more accurate CO<sub>2</sub> mass predictions from experiment 2 and 3 data (Figure 3), apparently due to variability in dye behavior between experiments. Small-scale experiments (data not shown) revealed that dye tended to flocculate at low pH, which could cause changes in dye concentration in the stock solution between experiments. This variability in concentration should affect the intensity, rather than the shape, of the predicted plume, which is evidenced in contour plots of experiments 2 and 3. Contour plots in Figures 4a and 4b were computed using the average  $k$  value, while those in Figures 4c and 4d were derived from individual  $k$  values. Using the individual  $k$  values did not markedly affect the overall plume geometry, which is similar between the two experiments, but did result in more similarly sized regions of high concentration.

[15] A number of the data transformation steps described above may present sources of error to the method. In step 1, the coefficients used to calculate water content were computed using a different filter and using water instead of dye solution, thus their accuracy for this application is uncertain. In step 2, the main source of error is the  $k$  calibration which was sensitive to dye variability, yielding a wide variety of  $k$  values. Dye variability also may contribute to error in step 3, where we found pH dye attenuation data at low pH to vary between replicates. This error could be largely eliminated through the use of a more soluble dye, and through more direct calibration in the chamber system.

[16] This imaging method enabled the visualization of the development and movement of a CO<sub>2</sub> plume through unsaturated porous media. The method was primarily hampered by dye behavior, which could be remedied with a more soluble pH indicator dye. The accuracy of the model might be improved by: recalibration of the water content equation to the dye solution over a range of pH values using Niemet and Selker's [2001] technique; and, reformulation of the dye attenuation equation to calculate solution pH directly from light intensity. Alternatively, one could use a blended CO<sub>2</sub>, with for example 50–90% N<sub>2</sub>. In this way one could adjust the equilibrium pH to avoid the solubility threshold observed here. Finally, one could test the formation of precipitates as a function of dye concentration.

[17] This new technique has many appealing features for the observation of gas flow in variably saturated porous media. It provides spatial resolution at the millimeter scale; provides temporal resolution of seconds; is nondestructive and noncontact; and in principle allows simultaneous observation of other key parameters such as liquid saturation, microbial distribution, and solute distribution. At present further research is needed in the area of the optimal concentrations of dye and CO<sub>2</sub> to be used, and simultaneous measurement of water content will require attention, either to assuring the observation of light transmitted is carried out at light wavelengths that are not effected by the changing dye color, or by calibration of the water content based on the observed dye color. The technique is also limited to use with gases such as CO<sub>2</sub> which alter the solution pH. Clearly buffered solutions, as may be required in biological experiments, would interfere with this technique, as might other alterations of media or liquid solutes. Hence the light transmission technique is shown to have the potential to be an important addition to the study of gas phase flow in unsaturated media, with direction for development indicated through interpretation of a set of laboratory experiments.

## References

- Butler, J. N. (1982), *Carbon Dioxide Equilibria and Their Applications*, Addison-Wesley, Boston, Mass.
- Hillel, D. (1998), *Environmental Soil Physics*, 2nd ed., Elsevier, New York.
- Niemet, M. R., and J. S. Selker (2001), A new method for quantification of liquid saturation in 2D translucent porous media systems using light transmission, *Adv. Water Resour.*, 24, 651–666.
- Rockhold, M. L. (2002), Interactions between microbial dynamics and transport processes in soils, Ph.D. dissertation, Oregon State Univ., Corvallis.
- Schroth, M. H., S. J. Ahearn, J. S. Selker, and J. D. Istok (1996), Characterization of Miller-similar silica sands for laboratory hydrologic studies, *Soil Sci. Soc. Am. J.*, 60, 1331–1339.
- Schroth, M. H., J. D. Istok, J. S. Selker, M. Ostrom, and M. D. White (1998), Multifluid flow in bedded porous media: Laboratory experiments and numerical simulations, *Adv. Water Resour.*, 22, 169–183.
- van Genuchten, M. T. (1980), A closed-form equation for predicting the hydraulic conductivity of unsaturated soils, *Soil Sci. Soc. Am. J.*, 44, 892–898.
- Weisbrod, N., M. R. Niemet, and J. S. Selker (2003), Light transmission technique for the evaluation of colloidal transport and dynamics in porous media, *Environ. Sci. Technol.*, 37, 3694–3700.
- Yarwood, R. R., M. L. Rockhold, M. R. Niemet, J. S. Selker, and P. J. Bottomley (2002), Noninvasive quantitative measurement of bacterial growth in porous media under unsaturated-flow conditions, *Appl. Environ. Microbiol.*, 68, 3597–3605.

L. Parker and J. Selker, Department of Bioengineering, 210 Gilmore Hall, Oregon State University, Corvallis, OR 97331-3609, USA. (selkerj@enr.orst.edu)

R. Yarwood, Department of Crop and Soil Sciences, Oregon State University, Corvallis, OR 97331, USA.